CASE FILE
COPY

NACA RM E53J06

NACA

RESEARCH MEMORANDUM

INVESTIGATION OF A HIGH-PRESSURE-RATIO EIGHT-STAGE AXIAL-FLOW RESEARCH COMPRESSOR WITH TWO TRANSONIC INLET STAGES

II - PRELIMINARY ANALYSIS OF OVER-ALL PERFORMANCE

By Richard P. Geye, Ray E. Budinger, and Charles H. Voit

Lewis Flight Propulsion Laboratory
Cleveland, Ohio

NATIONAL ADVISORY COMMITTEE
FOR AERONAUTICS

WASHINGTON

December 1, 1953
Declassified September 17, 1958

NATIONAL ADVISORY COMMITTEE FOR AERONAUTICS

RESEARCH MEMORANDUM

INVESTIGATION OF A HIGH-PRESSURE-RATIO EIGHT-STAGE AXIAL-FLOW RESEARCH COMPRESSOR WITH TWO TRANSONIC INLET STAGES

II - PRELIMINARY ANALYSIS OF OVER-ALL PERFORMANCE

By Richard P. Geye, Ray E. Budinger, and Charles H. Voit

SUMMARY

An investigation of the over-all performance of a 20-inch-tip-diameter, eight-stage axial-flow compressor was conducted as the initial step in an investigation of the problems encountered in a high-pressure-ratio axial-flow compressor with transonic inlet stages. The compressor was designed to obtain a total-pressure ratio of 10.26 (a root-mean total-pressure ratio per stage of 1.338) with an equivalent weight flow of 65.0 pounds per second (a specific weight flow of 29.8 (lb/sec)/sq ft of frontal area) at an equivalent tip speed of 1168 feet per second.

The investigation was made over a range of weight flows at equivalent speeds from 30 to 100 percent of design speed. The maximum total-pressure ratio obtained at design speed was 9.90 at an equivalent weight flow of 64.5 pounds per second with an adiabatic efficiency of 0.82. The maximum equivalent weight flow obtained at design speed was approximately 65 pounds per second. The peak efficiencies were high over much of the speed range investigated, remaining above 0.85 for equivalent speeds ranging from approximately 66 to 96 percent of design speed. A minimum peak efficiency of 0.73 was obtained at 30 percent of design speed; as the compressor speed increased, the peak efficiency increased to a maximum of approximately 0.88 between 80 and 90 percent of design speed and then decreased to 0.82 at design speed. The compressor surge line had a slight knee at approximately 63 percent of design speed; however, the knee is of minor proportions and the high part-speed efficiencies could result in good performance, starting, and accelerating characteristics for an engine requiring a design total-pressure ratio and equivalent weight flow somewhat below those for which the compressor was originally designed.

INTRODUCTION

In order to study the design and off-design performance problems of a high-mass-flow, high-pressure-ratio multistage compressor with both

transonic and subsonic stages, a 20-inch-tip diameter, eight-stage axial-flow compressor having two transonic inlet stages was designed and fabricated at the NACA Lewis laboratory. The compressor was designed to achieve higher stage total-pressure ratios (average of 1.338) and specific weight flows (29.8 (lb/sec)/sq ft of frontal area) than those in current use, while at the same time maintaining high efficiency (an assumed efficiency of 0.86 was used in design). Details of the compressor design are presented in reference 1.

As an initial phase of the investigation, the over-all performance characteristics were obtained over a range of equivalent speeds from 30 to 100 percent of design speed. This report discusses the over-all performance analysed on the basis of the following data: over-all total-pressure ratio, adiabatic temperature-rise efficiency, average compressor-discharge Mach number, and stage tip static-pressure ratio distribution through the compressor. In addition, the applicability of the compressor as an engine component is pointed out.

SYMBOLS

The following symbols are used in this report:

A	frontal area, sq ft
P	absolute total pressure, lb/sq ft
p	absolute static pressure, lb/sq ft
T	total temperature, $^{\circ}F$
W	weight flow, lb/sec
δ	ratio of inlet total pressure to NACA standard sea-level pressure
θ	ratio of inlet total temperature to NACA standard sea-level temperature

Subscripts:

n	station number
0	inlet depression-tank station
1,3,5, . . . 15	stations ahead of rotors of 1st, 2nd, 3rd, . . . 8th stages
2,4,6, . . . 16	stations ahead of stators of 1st, 2nd, 3rd, . . . 8th stages

17	station after 8th stator
18	station ahead of discharge vane
19	station after discharge vane
20	discharge measuring station

APPARATUS

Compressor. - A picture of the compressor is shown in figure 1, and a cross-sectional view of the compressor, the inlet bellmouth nozzle, and the discharge collector is shown in figure 2. The aerodynamic design details of the compressor are presented in reference 1 and result in the following design values:

Total-pressure ratio	10.26
Root-mean total-pressure ratio per stage	1.338
Equivalent weight flow, lb/sec	65.0
Equivalent weight flow, (lb/sec)/sq ft frontal area	29.8
Equivalent tip speed, ft/sec	1168
Adiabatic efficiency	0.862
Average compressor-discharge axial Mach number	0.358
Inlet hub-tip ratio	0.48

Installation. - The compressor was driven by a 9000-horsepower variable-frequency electric motor. The speed was maintained constant by an electronic control and was measured by an electric chronometric tachometer.

Air entered the compressor through a calibrated, adjustable submerged orifice, a butterfly inlet throttle, and a depression tank 6 feet in diameter and approximately 10 feet long. Screens in the depression tank and a smooth bellmouth nozzle faired into the compressor inlet were used to obtain a uniform distribution of air entering the compressor. Air was discharged from the compressor into a collector that was connected to the laboratory altitude exhaust system. Air weight flow was controlled by a butterfly valve located in the exhaust ducting. The compressor was insulated with 2 inches of glass wool in order to reduce the heat transfer through the casing.

Instrumentation. - The axial locations of the instrument measuring stations are shown in figure 2. The inlet depression-tank station and the compressor discharge station had axial locations that were in accordance with reference 2. As a result of an axial space of approximately 1.5 inches between the eighth-stage stator blades and the exit guide vanes, there were two interstage measuring stations between these

blade rows: station 17, approximately 0.25 inch behind the eighth-stage stators; and station 18, approximately 0.25 inch ahead of the exit guide vanes. This was the only case in which more than one interstage measuring station was located between adjacent blade rows. Radial distributions of total temperature and total pressure were obtained from multiple probe rakes located at the area centers of equal-annular areas. The instruments used at each station and the method of measurement were as follows:

Depression-tank pressure:
Four wall static-pressure taps and one total-pressure probe (velocity head negligible at this station)

Depression-tank temperature:
Four multiple-tip total-temperature probes

Compressor-inlet static pressure:
Four wall static-pressure taps located around the casing circumference and two located in the hub approximately 0.5 inch upstream of the first rotor

Compressor-blade-row static pressure:
Four wall static-pressure taps located around the casing circumference after each blade row

Compressor-discharge pressure:
Four wall static-pressure taps at the tip and two at the hub; three 10-tube circumferential total-pressure rakes (fig. 3(a)) located at the area centers of equal-annular areas. The circumferential length of a rake is greater than the circumferential distance between exit guide vanes.

Compressor-discharge temperature:
Four spike-type thermocouple rakes (fig. 3(b)) with three measuring stations located at area centers of equal-annular areas and outside of exit guide-vane wakes. These thermocouples are connected differentially with the depression-tank thermocouples.

Pressure measurement:
Mercury manometers

Temperature measurement:
Self-balancing potentiometers

The accuracy of measurement is estimated to be within the following limits: temperature, $\pm 1.0^{\circ}$ F; pressure, ± 0.05 in. Hg; weight flow, ± 1.5 percent; speed, ± 0.3 percent.

PROCEDURE

Operation. - The compressor was operated at equivalent speeds from 30 to 100 percent of design speed. At 30, 50, 60, 70, 80, 90, and 100 percent speed, the range of air flows investigated extended from a maximum flow to a flow at which incipient surge was encountered; at 55, 63, 65, 67, 75, and 95 percent speed, only the incipient-surge point was investigated. At all speeds except 30 and 50 percent of design speed, the inlet pressure was varied to maintain a constant Reynolds number (based on the blade chord at the tip of the first rotor and the air properties relative to the tip of the first rotor) of approximately 1,000,000. Atmospheric inlet air was used from 30 to 80 percent of equivalent design speed, and refrigerated inlet air was used at all equivalent speeds above 80 percent of design in order to reduce the outlet temperature and the mechanical speed of the compressor.

Calculations. - At each flow point the discharge total pressure was obtained by two methods: The measured discharge total pressure was the arithmetic average of three 10-tube circumferential rake measurements taken at the area centers of equal-annular areas. The calculated discharge total pressure was obtained by the method presented in reference 2. With this method a uniform discharge velocity in the axial direction was assumed; and the measured values of discharge static pressure, total temperature, weight flow, and area normal to the compressor axis were used to determine the discharge total pressure from the energy and continuity equations. Inasmuch as the assumptions of this method do not credit the compressor for discharge velocity gradients or deviation from axial discharge, the calculated values of discharge total pressure would be expected to be somewhat lower than the measured values. However, in reality, the discharge total pressure as determined by the two methods was approximately equal except at the high-flow low-pressure-ratio end of the individual speed curves where exceptionally large discharge velocity gradients existed. Because of this close correlation between the discharge total pressures as determined by both methods and because of the recommendations of reference 2, only the compressor total-pressure ratio as determined by the calculated discharge total pressure is presented in this report.

The calculated compressor total-pressure ratio was used to determine the isentropic power input; and the compressor temperature rise, obtained by taking the arithmetic average of differential temperatures measured between the compressor discharge and the inlet depression tank, was used to determine the actual power input from which the adiabatic temperature-rise efficiency was calculated.

RESULTS AND DISCUSSION

Over-all performance. - The over-all performance characteristics of the compressor are presented in figure 4 as a plot of total-pressure ratio, with the contours of constant efficiency, as a function of the equivalent weight flow. At design speed a maximum total-pressure ratio of 9.90 (root-mean total-pressure ratio per stage of 1.332) was obtained at an equivalent weight flow of 64.5 pounds per second (29.6 (lb/sec)/sq ft of frontal area) with an efficiency of 0.82; a peak efficiency of 0.82 was obtained at total-pressure ratios ranging from 8.46 to 9.90; and a maximum equivalent weight flow of approximately 65 pounds per second (29.8 (lb/sec)/sq ft of frontal area) was obtained.

The compressor surge line indicated in figure 4 has a slightly increasing slope up to approximately 63 percent of equivalent design speed. At approximately 63 percent of design speed, probably as the result of the first stages remaining out of stall as surge is approached at this and higher speeds (ref. 3), there is an abrupt increase in the slope of the surge line. This change in surge-line slope causes a slight knee in the surge line. At speeds above that at which the knee occurs, the slope of the surge line remains nearly constant.

The efficiency characteristics are presented in figure 5 with the adiabatic temperature-rise efficiency plotted as a function of equivalent weight flow. The peak efficiency has a minimum value of 0.73 at 30 percent of design speed; as the compressor speed is increased, the peak efficiency increases to a maximum of approximately 0.88 between 80 and 90 percent of design speed and then decreases to 0.82 at design speed. The peak efficiencies are high over much of the speed range investigated, remaining above 0.85 for equivalent speeds ranging from approximately 66 to 96 percent of design speed. In addition, the constant-efficiency contours (fig. 4) include a wide range of pressure ratios at a given speed.

The average compressor-discharge Mach number is presented in figure 6 plotted as a function of equivalent weight flow. The surge line represents the minimum average discharge Mach numbers at which the compressor can operate over the range of equivalent speeds investigated. As the compressor speed is increased, the average discharge Mach number at the surge line increases from a value of 0.17 at 30 percent of design speed to a maximum of 0.33 at 63 percent of design speed (the speed and weight flow at which the knee occurs in the surge line of fig. 4). At 63 percent of design speed, the average discharge Mach number at surge reverses its trend and decreases to a value of 0.27 at design speed.

Stage performance. - A typical curve of static-pressure ratio for a single-stage compressor is plotted in figure 7 as a function of equivalent weight flow. The direction of increasing angle of attack and

positive stall is to the left of the peak-pressure-ratio point, and the direction of decreasing angle of attack and negative stall is to the right. In multistage compressor design, the blading for each stage at the design point is usually selected to operate at the peak-efficiency point of the stage performance curve, as indicated in figure 7.

The representative stage performance curves are presented in figure 8 as a plot of stage static-pressure ratio (based on outer-casing-wall static pressures) against equivalent weight flow. The operating range of the various stages obtained at each speed can be considered as a segment, uncorrected for speed, of the typical stage performance curve presented in figure 7. As indicated in figure 8(a) the inlet stage operates on the positive stall side of the peak-pressure-ratio point at speeds up to and including 60 percent of design speed and near the peak-pressure-ratio point at 70 percent of design speed. At 80 and 90 percent of design speed, the inlet stage is operating in the range of the peak-efficiency point; and at design speed its range of operation has moved down on the negative stall side of the stage performance curve.

Figure 8(b) indicates that the intermediate stage (fourth), at speeds up to and including 60 percent of design speed, operates in the range of the peak-pressure-ratio point (fig. 7); at speeds greater than 60 percent of design, the range of operation shifts toward the negative stall side of the stage performance curve with the stage operating near the peak-efficiency point (fig. 7) at 70, 80, and 90 percent of design speed.

It is apparent from figure 8(c) that a change in weight flow at a given speed causes the eighth stage to operate over a much larger segment of the complete stage performance curve (over a much wider range of angles of attack) than it does the first or fourth stage (ref. 4). Up to 80 percent of design speed a reduction in weight flow at a given speed moves the operating point of the eighth stage up the negative stall side of the performance curve toward the peak-pressure-ratio point; at 90 and 100 percent of design speed a reduction in weight flow moves the eighth-stage operating point to the peak-pressure-ratio point and onto the positive stall side of the performance curve.

From figure 8 it is apparent that over a certain range of equivalent weight flows at 80 and 90 percent of equivalent design speed the representative stages are very well matched (operate simultaneously near their peak-efficiency points (fig. 7)). As a result, over-all peak efficiencies of approximately 0.87 (fig. 5) were obtained at these speeds. From a consideration of over-all pressure ratio, efficiency, and mass flow attainable, the best match point would probably be at about 90 percent of equivalent design speed with a total-pressure ratio of about 7.5.

Comparison with design. - The values of the ratio of tip static pressure at each station to the compressor-inlet total pressure, together with the tip static-pressure ratios across each stage and blade row, were obtained at the design-speed surge point, the point nearest the design total-pressure ratio at design speed, and are compared with the design-point pressure-ratio values in figure 9. The actual values of the ratio of tip static pressure at each station to the inlet total pressure deviate by as much as 12 percent from the design values; however, the actual value leaving the eighth stator is equal to the design value, indicating that the design static pressure was attained at the compressor discharge. In the case of the stage tip static-pressure ratios, the maximum deviation from design is approximately 9 percent with the first two stages having static-pressure ratios below design, the middle four stages having static-pressure ratios above design, and the last two stages being approximately on design. The blade-row static-pressure ratios also have a maximum deviation from design of approximately 9 percent, with the stator-row static-pressure ratios being less than design in all but the third stage and the rotor-row static-pressure ratios being greater than design in all but the first two stages. This comparison of static-pressure ratio distribution gives some indication as to the work being done by the various stages near the design point; but it does not indicate the position at which each stage is operating with respect to its peak-pressure-ratio point or how well the various stages are matched.

Some indication of this can be obtained from figure 8, which was previously presented in the discussion of stage performance. At the design-speed surge point (solid symbol in fig. 8), the point nearest the design total-pressure ratio, good stage matching was expected; however, it is apparent from figure 8 that the first and eighth stages are mismatched at this point. As a result of this mismatch, the design total-pressure ratio was not attained at design speed and the maximum efficiency was lower than that obtained at 90 percent of design speed.

From the data available it appears that the mismatching at the design-speed maximum-pressure ratio (surge point) was probably the result of the following: (1) improper selection of the optimum angle of incidence in the transonic stages, (2) improper assumption of area correction for boundary-layer growth, and (3) insufficient camber in certain stages.

The design equivalent weight flow was attained at design speed (fig. 4); thus, the first-stage transonic rotor should be operating at the angle of incidence intended in design. However, as seen in figure 8(a), the first transonic stage is operating down on the negative stall side of its performance curve at the design-speed maximum pressure ratio. This indicates that the meager design information available at the time the compressor was designed led to the selection of a low optimum angle of incidence for the first transonic stage and possibly the second.

At the design-speed maximum pressure ratio, the average discharge Mach number was only 0.27 (fig. 6); whereas, the average design discharge Mach number was 0.358. Inasmuch as the design discharge static pressure and essentially the design mass flow were obtained at the design-speed maximum-pressure ratio, it is apparent that, in design, there was an overcompensation for boundary-layer growth through the compressor which resulted in axial velocities below those intended in the latter stages of the compressor. Consequently, the angle of attack in the eighth stage (and probably other rear stages) is greater than that intended in design; and as indicated in figure 8(c), the stage operates on the positive stall side of its performance curve at the design-speed maximum pressure ratio.

The angle of attack and camber of the subsonic rotor blades were selected (ref. 1) from the cascade design point, and hence it would be expected that the peak static-pressure ratio would be appreciably higher than the design static-pressure ratio. However, the actual static-pressure ratio obtained in the eight-stage compressor (fig. 8(c)) was only slightly higher than design. From this it appears that the entire stage operating curve has been shifted to a lower pressure-ratio level than was intended in design. This indicates that the blading in this stage may have insufficient camber to provide the turning and pressure rise desired at a given angle of attack.

Engine application. - Altitude operation at cruising flight speeds requires compressor equivalent speeds higher than at sea-level conditions; consequently, it is desirable to maintain high efficiency at overspeed. From the design-speed characteristics of this compressor, it is apparent that a turbine matched at this compressor speed would probably result in an engine with poor overspeed characteristics.

In view of this probability the best match point for a turbine to produce an engine with good altitude operating characteristics appears to be somewhere along the 90-percent speed line. At such a match point an efficiency of approximately 0.87, an equivalent weight flow of approximately 27 pounds per second per square foot of frontal area, and a total-pressure ratio in the range of 6.5 to 7.5 could be attained with good overspeed characteristics.

A typical engine operating line having its design point at 90 percent of design speed and at a total-pressure ratio of 7.5 is superimposed on the over-all performance curves of the compressor in figure 10. This operating line was obtained by use of the general equations for compressor and turbine matching. These equations required that continuity be satisfied through the engine, that the turbine power must be equal to that required to drive the compressor, and that the pressure rise through the inlet diffuser and compressor must equal the pressure drop through the burner, turbine, and jet nozzle. A limiting turbine-inlet temperature of 2150° R was selected at the assumed design point, and a ratio of jet-nozzle area to turbine-nozzle area was determined. For operation at equivalent compressor speeds below the assumed design speed, this area

ratio is held constant; for operation at equivalent compressor speeds above the assumed design speed, the limiting turbine-inlet temperature is held constant.

The operating line lies approximately along the locus of the peak-efficiency points and appears to have some pressure-ratio margin for acceleration near the knee of the surge line. Thus, in spite of the slight knee in the surge line, the high-part-speed performance provides a compressor with operating characteristics which, when properly matched with a turbine, could produce an engine with good starting, accelerating, and performance characteristics.

Compressor-discharge characteristics are such that acceptable combustor performance should be attainable. Figure 11 presents the variation in compressor-discharge Mach number with circumferential and radial position. This figure indicates that there are no regions having extremely high Mach numbers, and the Mach number variation which exists would probably be reduced to some degree in passing through a diffuser to the burner. Combustor research (ref. 5) indicates that combustor efficiency improves with increasing values of inlet static pressure and total temperature and with decreasing values of velocity. Along the typical operating line (fig. 12) the average discharge Mach numbers are relatively low; and with a practical diffuser to reduce the burner inlet velocities still further, the high static pressure and total temperature at the outlet of the compressor should produce acceptable burner performance.

SUMMARY OF RESULTS

The following results were obtained from an investigation of overall performance of an eight-stage axial-flow compressor:

1. The maximum total-pressure ratio obtained at design speed was 9.90 at an equivalent weight flow of 64.5 pounds per second with an adiabatic efficiency of 0.82.

2. A peak efficiency of 0.82 was obtained at design speed at values of total-pressure ratio varying from 8.46 to 9.90.

3. A maximum equivalent weight flow of approximately 65 pounds per second was obtained at design speed.

4. The peak efficiency remained above 0.85 for equivalent speeds ranging from approximately 66 to 96 percent of design speed.

5. A minimum peak efficiency of 0.73 was obtained at 30 percent of design speed; as the compressor speed increased, a maximum peak efficiency of approximately 0.88 was obtained between 80 and 90 percent of design speed.

6. The compressor surge line had a slight knee at approximately 63 percent of design speed.

7. Static-pressure data indicated that the first and last stages are mismatched (the first stage operating near negative stall and the last stage operating on the positive stall side of its peak-pressure-ratio point) at the design-speed maximum pressure ratio.

Lewis Flight Propulsion Laboratory
National Advisory Committee for Aeronautics
Cleveland, Ohio, October 7, 1953

REFERENCES

1. Voit, Charles H.: Investigation of a High-Pressure-Ratio Eight-Stage Axial-Flow Research Compressor with Two Transonic Inlet Stages. I - Aerodynamic Design. NACA RM E53I24, 1953.

2. NACA Subcommittee on Compressors: Standard Procedures for Rating and Testing Multistage Axial-Flow Compressors. NACA TN 1138, 1946.

3. Budinger, Ray E., and Serovy, George K.: Investigation of a 10-Stage Subsonic Axial-Flow Research Compressor. IV - Individual Stage Performance Characteristics. NACA RM E53C11, 1953.

4. Huppert, Merle C., and Benser, William A.: Some Stall and Surge Phenomena in Axial-Flow Compressors. Paper presented at Inst. Aero. Sci. meeting, New York (N. Y.), Jan. 26-29, 1953.

5. Olson, Walter T., and Childs, J. Howard: NACA Research on Combustors for Aircraft Gas Turbines. I - Effect of Operating Variables on Steady-State Performance. NACA RM E50H31, 1950.

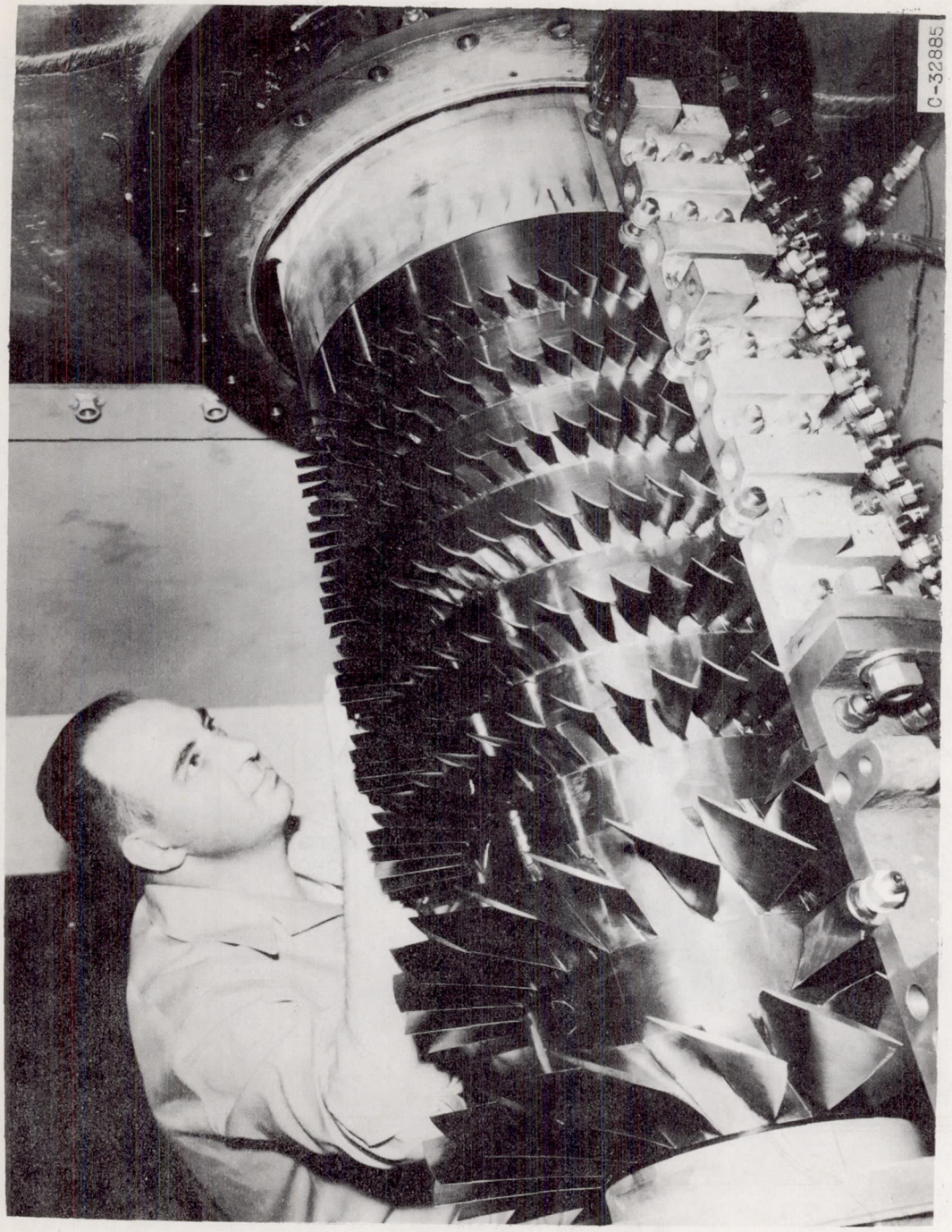

Figure 1. - Eight-stage axial-flow compressor.

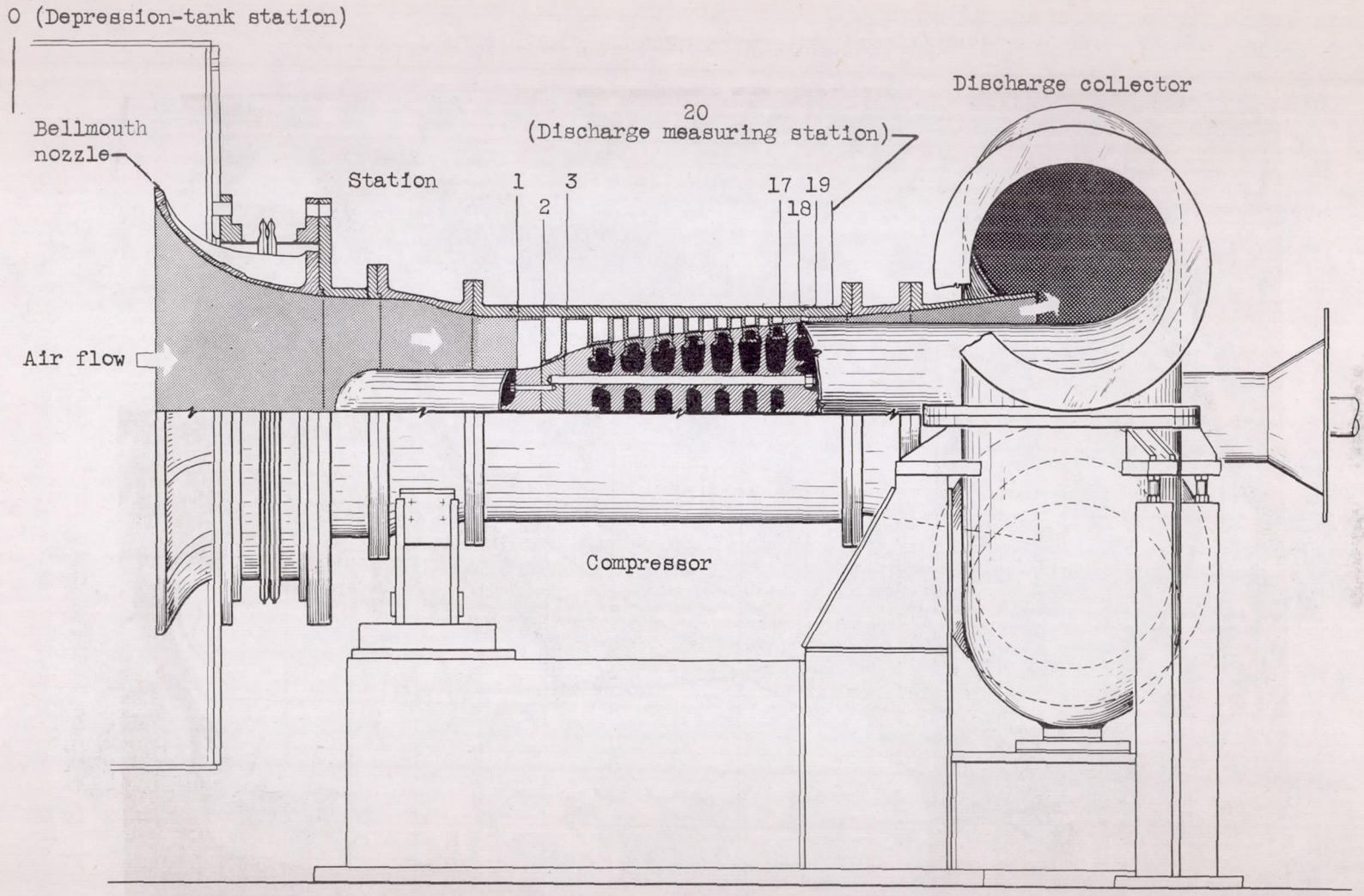

Figure 2. - Cross-sectional view of eight-stage axial-flow compressor, inlet bellmouth nozzle, and discharge collector.

CD-3180

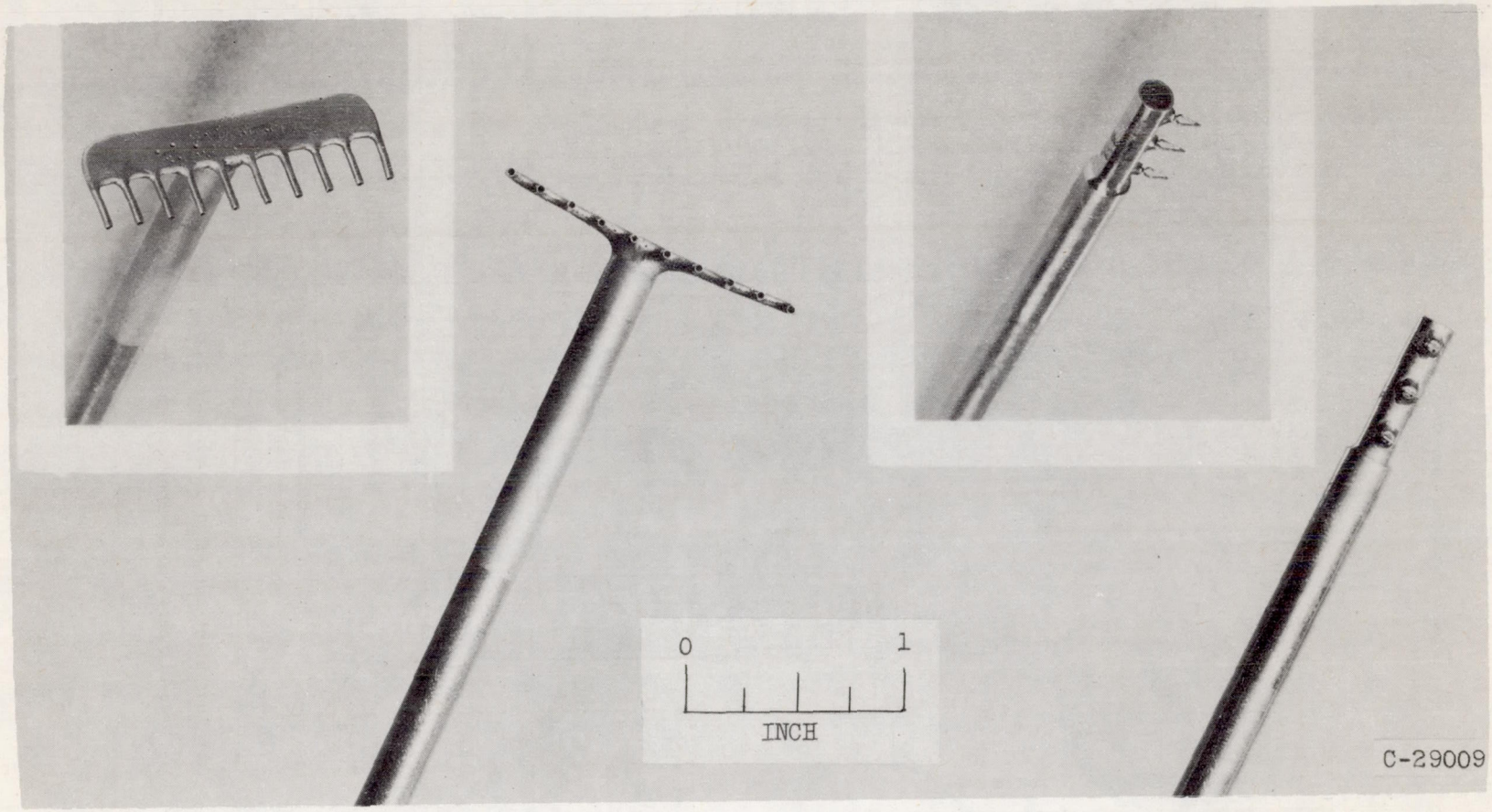

(a) Total-pressure rake.

(b) Spike-type thermocouple rake.

Figure 3. - Compressor-discharge instrumentation.

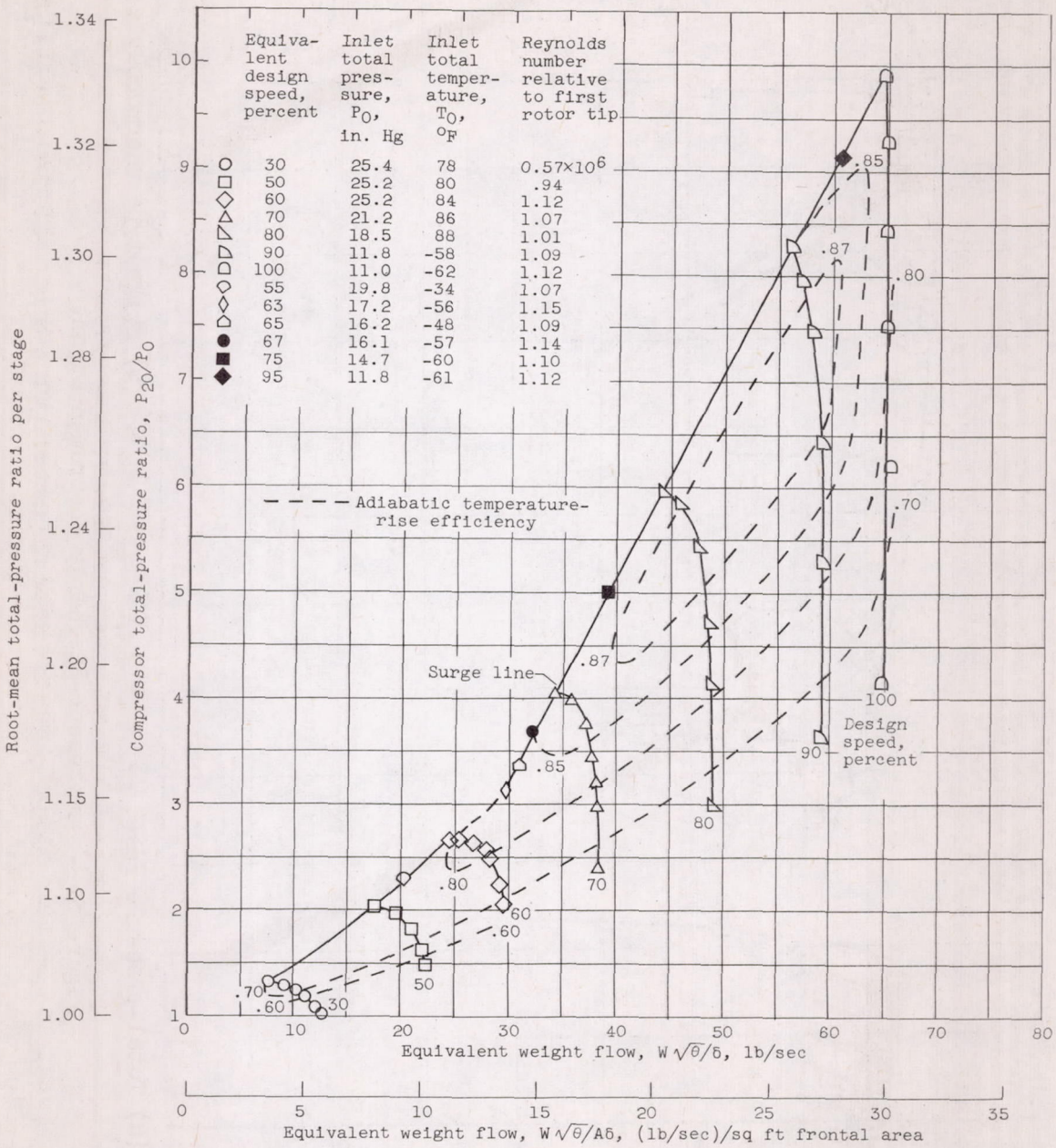

Figure 4. - Over-all performance characteristics of eight-stage axial-flow compressor.

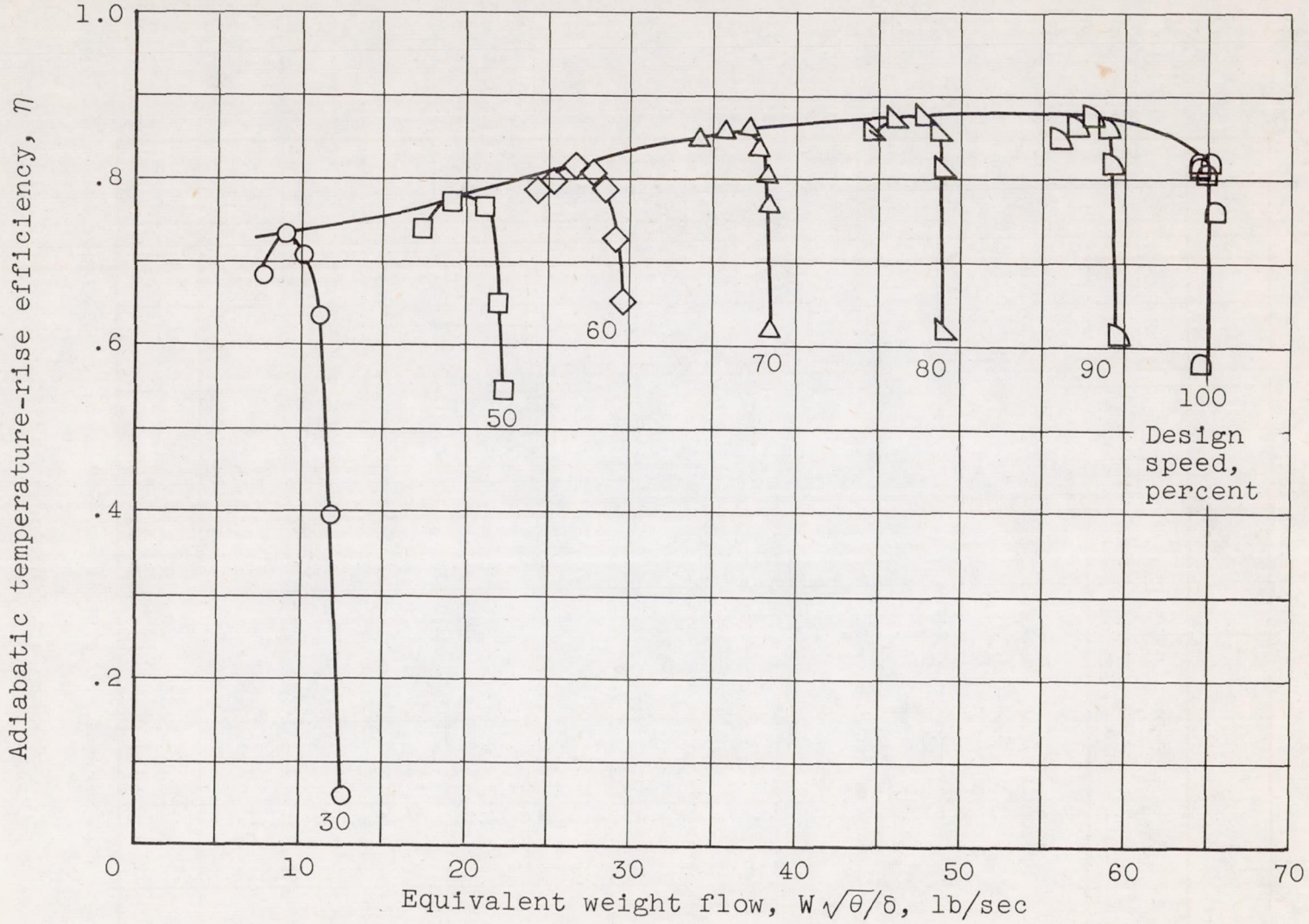

Figure 5. - Variation of adiabatic temperature-rise efficiency with speed and weight flow.

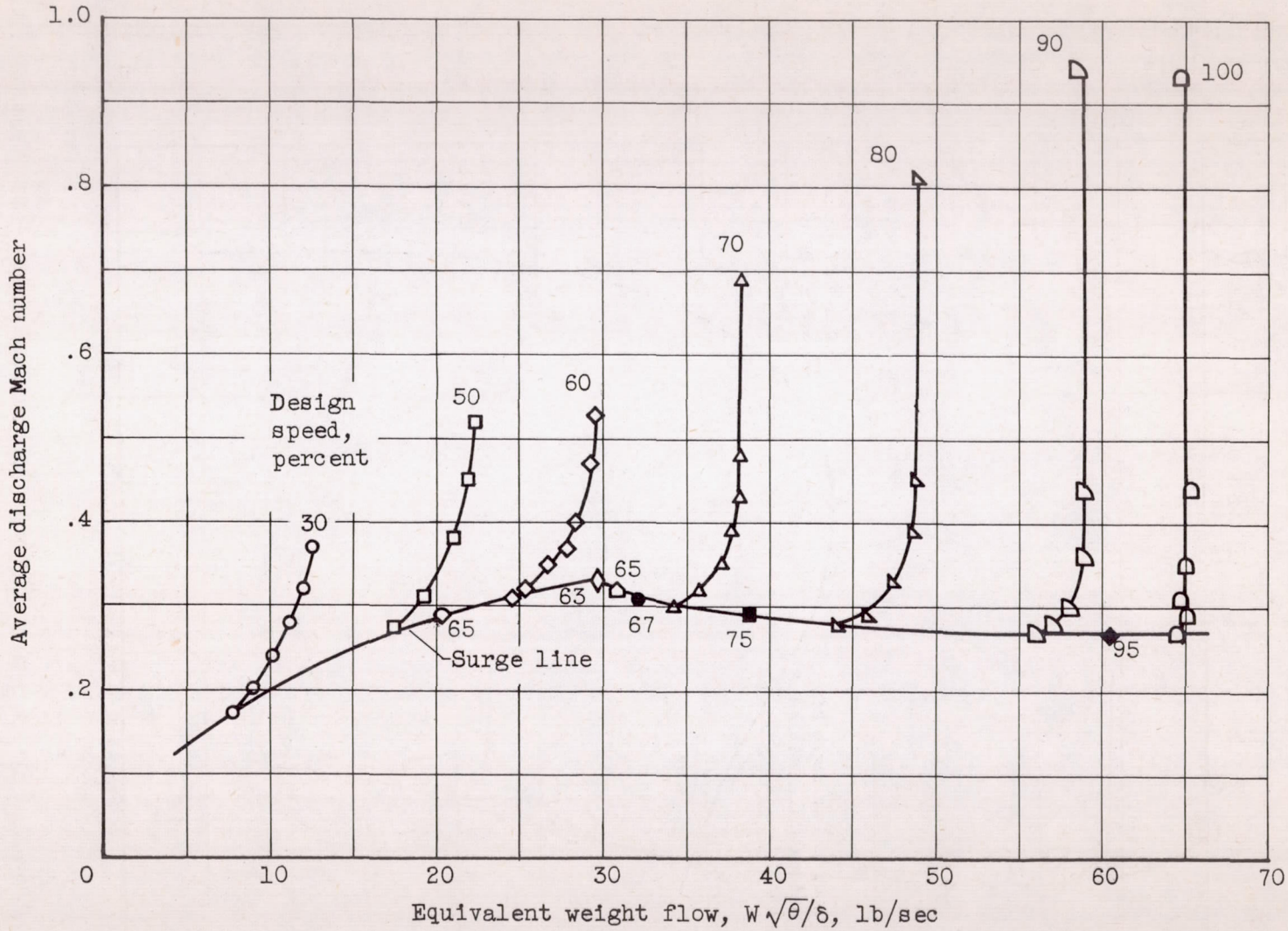

Figure 6. - Variation of average compressor discharge Mach number with speed and weight flow.

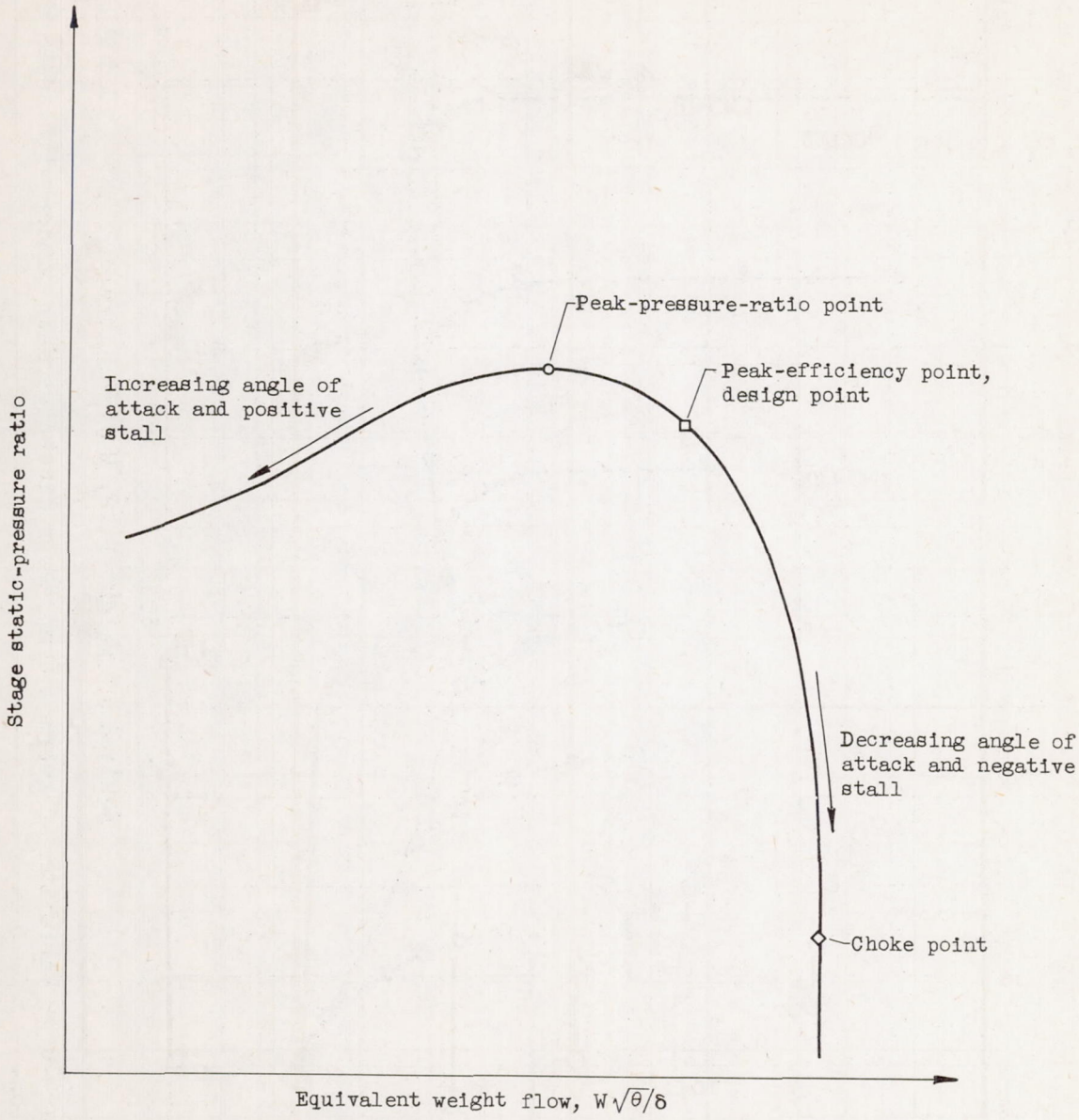

Figure 7. - Typical stage performance curve.

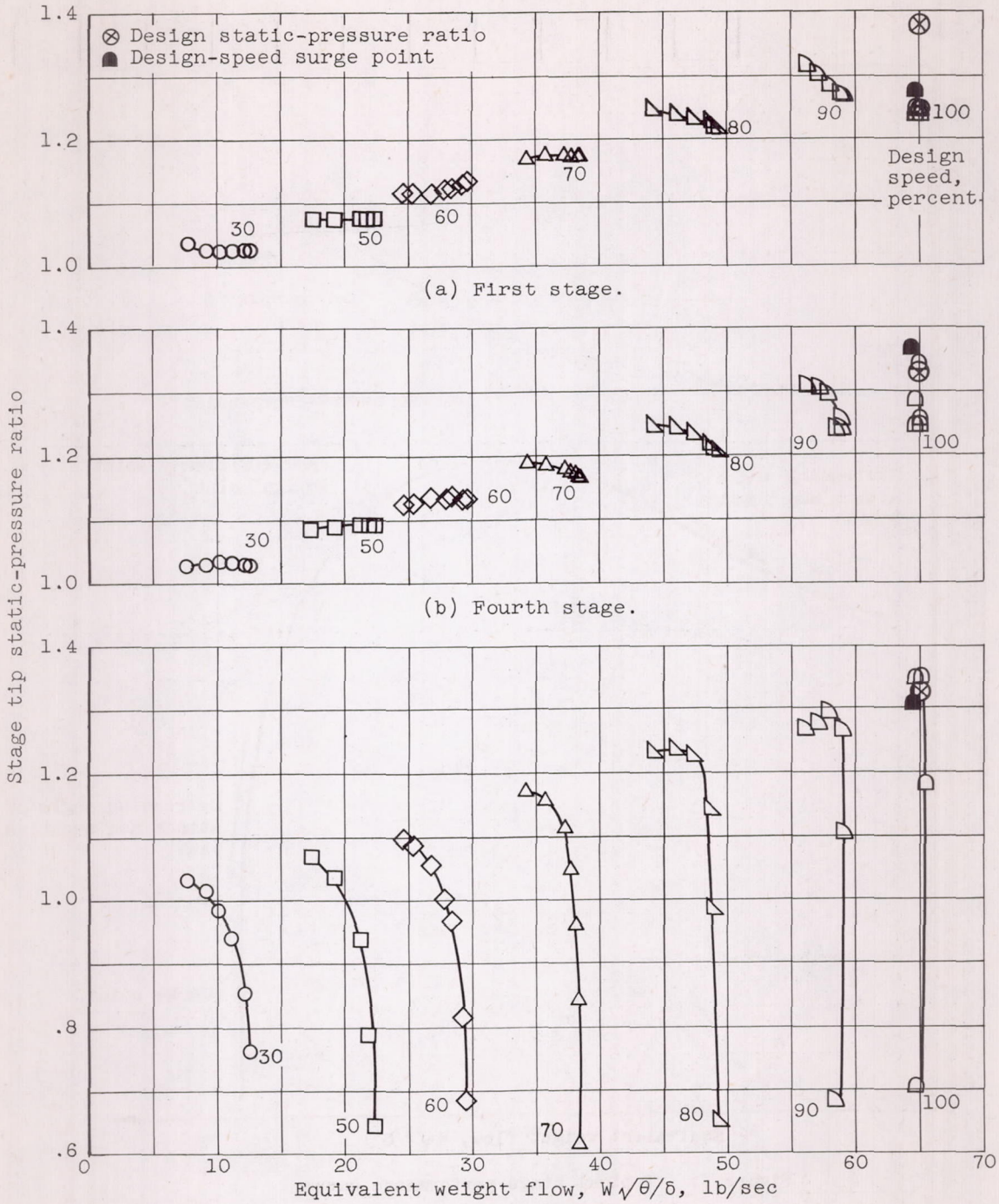

(c) Eighth stage.

Figure 8. - Variation of stage tip static-pressure ratio across first, fourth, and eighth stages with speed and weight flow.

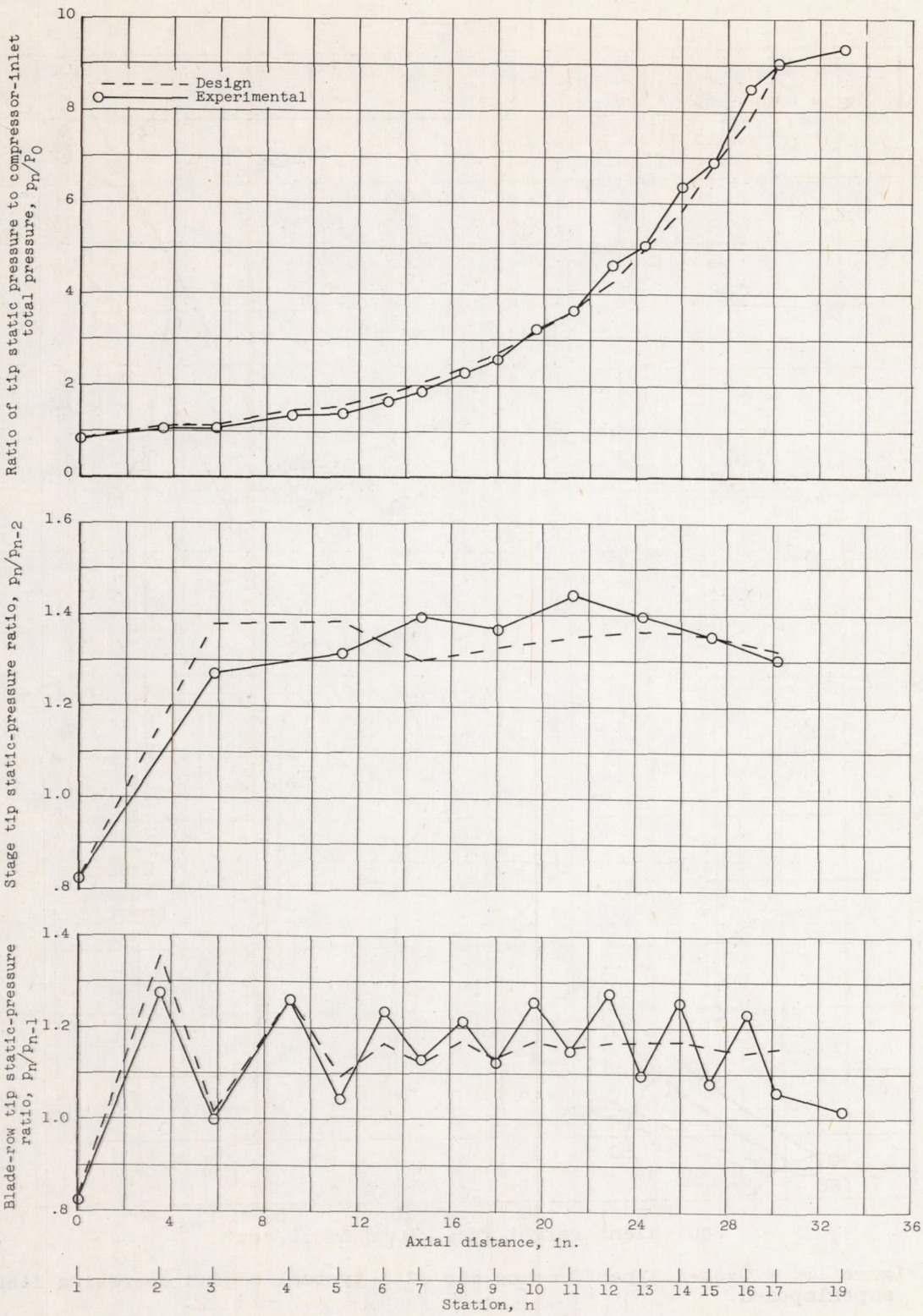

Figure 9. - Comparison with design of tip static-pressure ratio distribution obtained at 100-percent design-speed surge point.

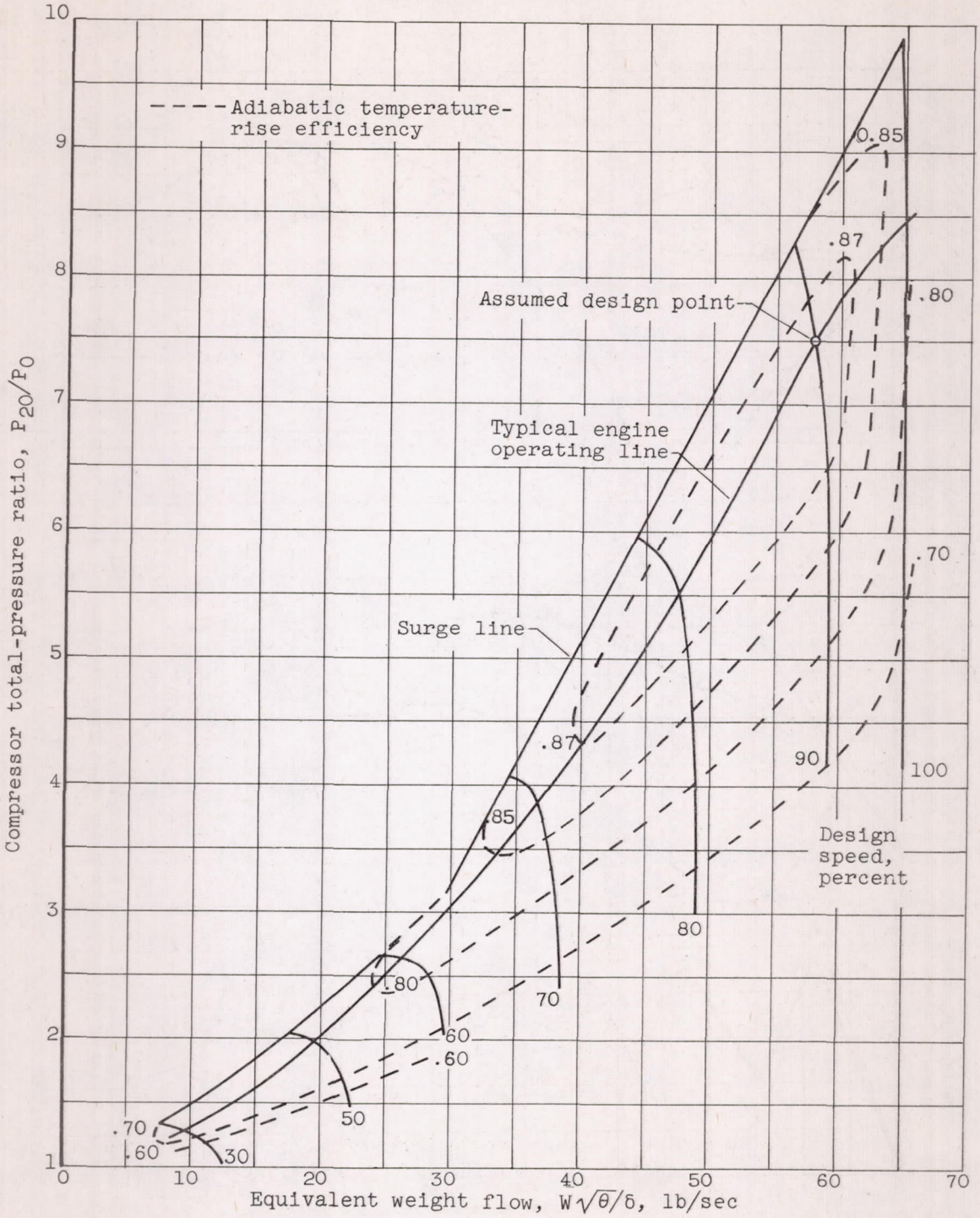

Figure 10. - Over-all performance map with typical engine operating line superimposed.

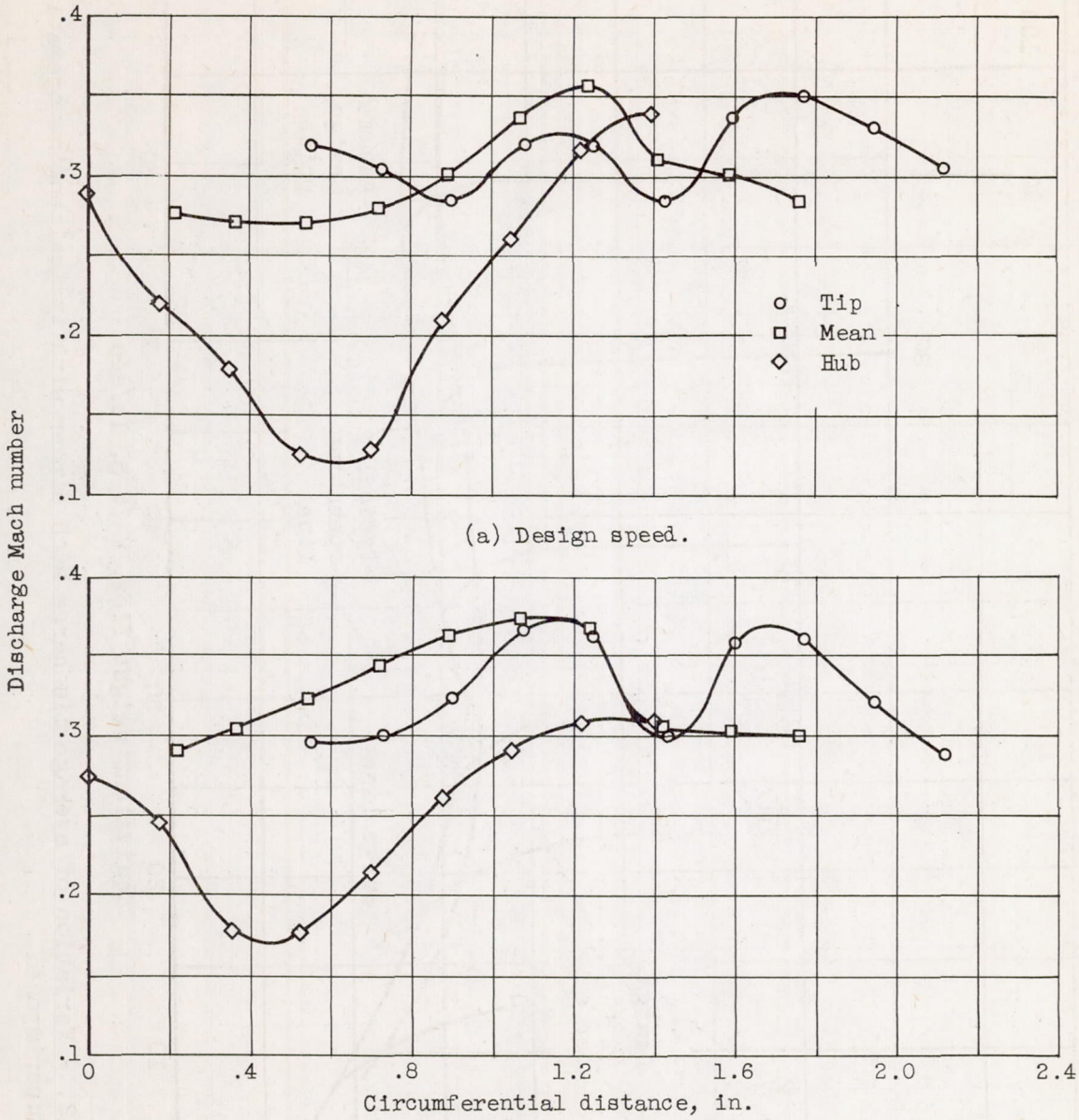

(a) Design speed.

(b) 90 Percent of design speed.

Figure 11. - Variation of compressor-discharge Mach number with radial and circumferential position for maximum-efficiency points at 90 and 100 percent design speed.

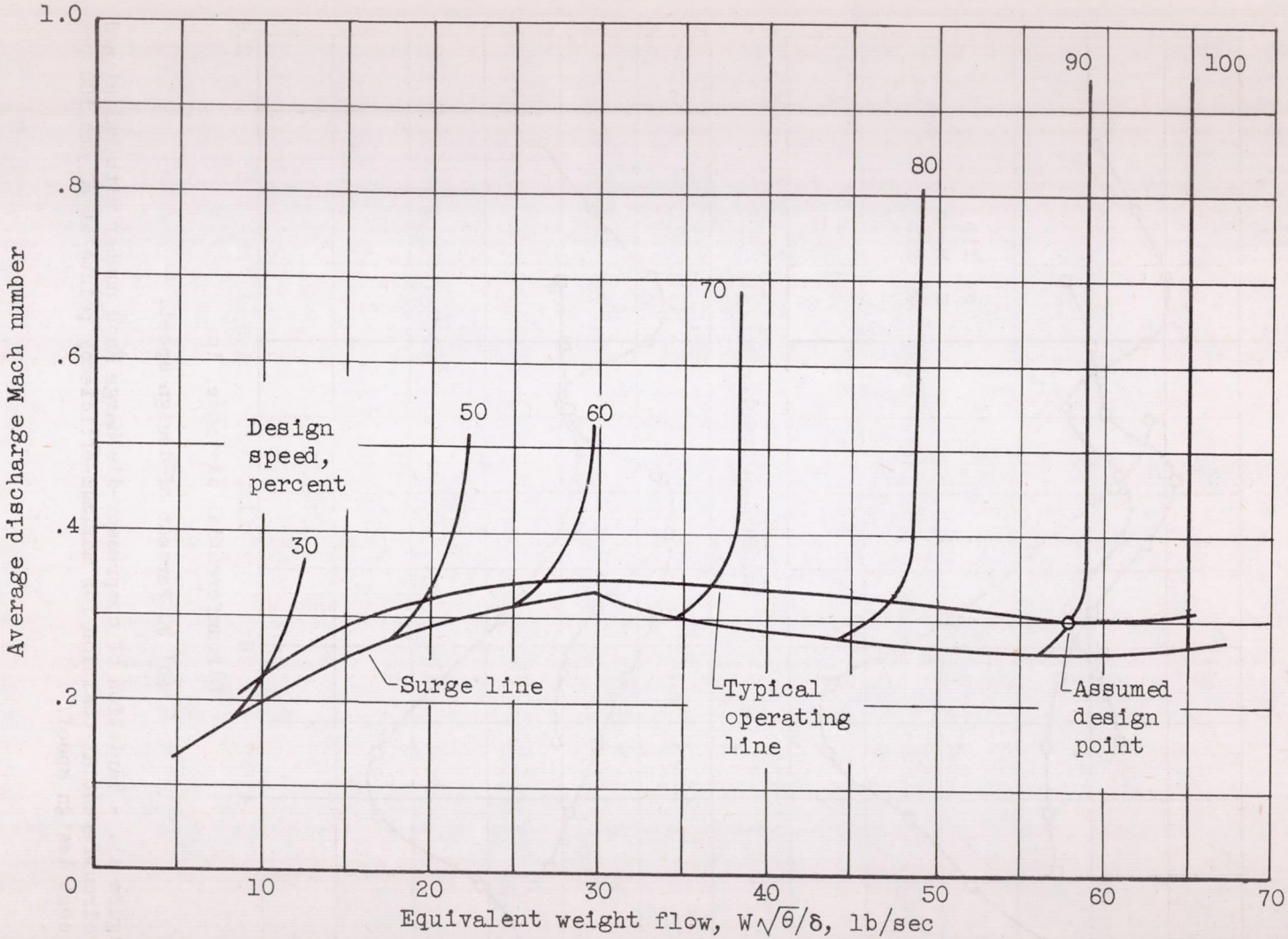

Figure 12. - Variation of average discharge Mach number with typical engine operating line superimposed.

NACA-Langley